ASD-TDR-63-699

Thermal Insulations for Aerospace Applications: -423° to +3000°F

M. L. Minges, 1st Lt, USAF

TECHNICAL DOCUMENTARY REPORT NO. ASD-TDR-63-699

September 1963

presented at

ASD 1963 Science and Engineering Symposium

Aeronautical Systems Division
Air Force Systems Command
Wright-Patterson Air Force Base, Ohio

NOTICES

When Government drawings, specifications, or other data are used for any purpose other than in connection with a definitely related Government procurement operation, the United States Government thereby incurs no responsibility nor any obligation whatsoever; and the fact that the Government may have formulated, furnished, or in any way supplied the said drawings, specifications, or other data, is not to be regarded by implication or otherwise as in any manner licensing the holder or any other person or corporation, or conveying any rights or permission to manufacture, use, or sell any patented invention that may in any way be related thereto.

Qualified requesters may obtain copies of this report from the Defense Documentation Center (DDC), (formerly ASTIA), Cameron Station, Bldg. 5, 5010 Duke Street, Alexandria 4, Virginia

This report has been released to the Office of Technical Services, U.S. Department of Commerce, Washington 25, D.C., in stock quantities for sale to the general public.

Copies of this report should not be returned to the Aeronautical Systems Division unless return is required by security considerations, contractual obligations, or notice on a specific document.

700 - December 1963 - 162-20-336

FOREWORD

Each year the Aeronautical Systems Division (ASD), Air Force Systems Command (AFSC), sponsors a Science and Engineering Symposium in advance of the Annual Air Force Science and Engineering Symposium. This provides a specific motivation for ASD personnel to prepare papers that reflect the results of their efforts. The variety of subjects also provides an opportunity for interdisciplinary exchange of information that is becoming ever more important.

This year the symposium papers are being published individually to facilitate distribution and retention. However, each paper carries this same foreword which lists the titles of all papers together with the authors and the ASD Technical Documentary Report (TDR) numbers. Readers who are interested in obtaining copies of other papers are urged to contact the authors directly or the Defense Documentation Center, Alexandria, Virginia. It should be noted that certain papers are classified and are available to only those persons having proper security clearances and a "need-to-know."

This paper is one of 21 presented at the "ASD 1963 Science and Engineering Symposium" held at Wright-Patterson Air Force Base, Ohio, 18-19 September 1963. They consist of 17 CONTRIBUTED and 4 INVITED papers, listed below. *The 5 contributed papers that are asterisked were also presented at the 10th Annual Air Force Science and Engineering Symposium held at the Air Force Academy, Colorado Springs, Colorado on 8, 9 and 10 October 1963.

CONTRIBUTED PAPERS

*Operation Fishbowl — Close-In Thermal Measurements, UNCLASSIFIED Title, SECRET-RESTRICTED DATA Paper
F. D. Adams
ASD-TDR-63-691

Radiation Physics: Its Impact on Instrumentation
R. C. Beavin, 1st Lt, USAF
ASD-TDR-63-697

*Application of Aerodynamic Lift in Accomplishing Orbital Plane Change
R. N. Bell, 1st Lt, USAF and W. L. Hankey, Jr., Ph. D.
ASD-TDR-63-693

Controlled Thermonuclear Reactions for Space Propulsion
R. F. Cooper and R. L. Verga
ASD-TDR-63-696

Comparison of Approaches for Sonic Fatigue Prevention
M. J. Cote
ASD-TDR-63-704

Air/Ground Communications Via Orbiting Reflectors
C. C. Gauder
ASD-TDR-63-702

*Ring Laser Techniques for Angular Rotation Sensing
D. A. Guidice and W. L. Harmon
ASD-TDR-63-694

Zero Gravity Pool Boiling
L. M. Hedgepeth and E. A. Zara
ASD-TDR-63-706

An Analytical Study on Liquid Cesium Purification in View of Current and Projected Needs
R. H. Herald
ASD-TDR-63-703

*Preliminary Weight Estimates for Advanced Dynamic Energy Conversion Systems
G. D. Huffman
ASD-TDR-63-705

Force Balance Determination of Inlet Performance for Advanced Vehicle Applications to Orbital Velocities Using Internal Drag Measurements
P. H. Kutschenreuter, Jr.
ASD-TDR-63-701

Thermal Insulations for Aerospace Applications: -423° to + 3000°F
M. L. Minges, 1st Lt, USAF
ASD-TDR-63-699

The Rankine Cycle Air Turboaccelerator (RATA) Engine — A New Cryogenic Engine system, UNCLASSIFIED Title, CONFIDENTIAL Paper
H. E. Pope
ASD-TDR-63-692

How PERT is Used in Managing the X-20 (Dyna-Soar) Program
R. M. Sadow
ASD-TDR-63-698

Liquid Metal Magnetohydrodynamic Power Conversion
G. B. Stafford
ASD-TDR-63-700

System Components Information Center
M. G. Toll
ASD-TDR-63-695

*Aerospaceplane — An Advanced System Planning Study,
UNCLASSIFIED Title, SECRET Paper
Alan Watton
ASD-TDR-63-690

The following four invited papers were prepared by the listed authors covering Air Force effort in the subject areas and were presented at the 10th Annual Air Force Science and Engineering Symposium. Copies of these papers may also be obtained from the authors or the Defense Documentation Center.

ASD-TDR-63-699

INVITED PAPERS

Summary of Laminar Flow Control Techniques for Aircraft
P. P. Antonatos, R. X. Mueller and J. P. Nenni
ASD-TDR-63-689

Materials for the Space Age
H. D. Colwick, Capt, USAF, D. H. Cartolano and C. W. Douglass
ASD-TDR-63-688

V/STOL Systems Technology Today and Tomorrow, UNCLASSIFIED Title, SECRET Paper
G. E. Dausman, Joseph Jordan and W. A. Summerfelt
ASD-TDR-63-687

Limited War/COIN, UNCLASSIFIED Title, SECRET Paper
D. A. Rook, Capt, USAF
ASD-TDR-63-686

A large percentage of the above listed authors are with organizational elements that have been or are being transferred from ASD to the recently established Research and Technology Division (RTD). These scientists and engineers from the Air Force Aero-Propulsion Laboratory, Air Force Avionics Laboratory, Air Force Flight Dynamics Laboratory, Air Force Materials Laboratory, and the Systems Engineering Group have, in some cases, prepared the symposium presentations as well as the published documents jointly with technical personnel remaining in ASD.

These 21 papers represent only a small portion of the ASD/RTD effort which spans from basic research through engineering and includes various aspects of technical management. They are illustrative of the competence of our technical personnel and we proudly dedicate them to all our scientists and engineers.

John E. Keto

JOHN E. KETO
Chief Scientist
Aeronautical Systems Division

BIOGRAPHY

LIEUTENANT M. L. MINGES was born in Denver, Colorado, in September 1937. He received a B.Sc. degree in chemical engineering from the Massachusetts Institute of Technology in 1959 and an M.Sc. degree in chemical engineering from the same University in 1960. Part of his graduate studies were completed at the MIT facility in Oak Ridge, Tennessee, including work in radiation chemistry, heat transfer, and reactor design at Oak Ridge National Laboratories. He entered the United States Air Force in August 1960 and was assigned to the AF Materials Laboratory where he has been engaged in thermal property research programs on cryogenic and high temperature materials. He is a Group Leader within the Specialty Materials Section.

Lieutenant Minges is attending Ohio State University pursuing studies that will lead to a Ph.D. degree in chemical engineering. He is a member of the American Institute of Chemical Engineers.

ABSTRACT

Very recent advances in thermal insulation developments for the temperature range from liquid hydrogen (-423°F) to +3000°F are reviewed. Some fundamental discussion of convective, conductive, and radiative heat transport mechanisms over this wide temperature range is included in analyzing the observed thermal characteristics of various insulation materials and composites. Variations in overall thermal conductance as a function of such parameters as absolute temperature level, interstitial gas pressure, density, radiation scattering and attenuation, and insulation geometry are discussed for recently developed powders, fibers, foams, and multilayer composites. Recent experimental results of USAF programs on these types of materials are presented and analyzed.

TABLE OF CONTENTS

LIST OF ILLUSTRATIONS

INTRODUCTION

In the development of vehicle and weapons systems which can operate dependably in both atmospheric and extra-terrestrial environments, high efficiency thermal insulations are an essential requirement. If cryogenic propellants are used in such high performance weapons systems, temperature extremes from liquid hydrogen (-423°F) to well above 3000°F may be encountered. Because of this fact the thermal insulation assumes such a vital role that in some instances overall system configurations may be dictated by insulation performance.

Functionally, there are two basic types of thermal insulation; first, those that rely entirely on inherent low thermal conductivity -- high thermal inertia characteristics in providing thermal protection -- so-called passive insulations; second, those that employ dynamic heat absorption in providing thermal protection -- so-called active insulations. Common examples of active insulations are, of course, those which make use of ablation and transpiration.

Depending on the magnitude of the incident heat flux and associated temperature levels, passive insulation approaches may be more efficient than those of active insulation. The form of the relationship is shown in Figure 1 (Ref. 1), where the thermal efficiency expressed as the absorption capacity per pound of insulation, is plotted as a function of the maximum heating rate, for an integrated heat load of 50,000 BTU/ft^2. Two important observations can be made from the Figure. First, as the maximum heating rate increases, overall thermal efficiency of all the insulation systems decreases. Secondly, at the lower maximum heating rates, passive insulation systems definitely come into favorable consideration. Further, these types of insulations are of relatively high thermal efficiency.

As manned lifting-body reentry systems become more advanced, the trend will be toward flight profiles with lower level heat fluxes of long duration. The trend can be illustrated by a comparison of current systems such as Mercury and Dyna-Soar. The basic difference is of course their reentry lift-drag ratios (L/D) which range from near zero to about 2.5, respectively. Heating times are short for the ballistic reentry systems and increase as the L/D ratio increases. Thus, for a constant, integrated heat flux of about 50,000 BTU/ft^2 the maximum heating rate for a ballistic reentry system (L/D $\cong$ 0) is an order of magnitude higher than that encountered by a controlled reentry system with L/D = 2.5 (Ref. 26). These facts and Figure 1 make clear that passive insulation materials are promising candidates for incorporation in lifting-body thermal protection systems.

In this report we consider some of the most recent developments in passive insulation materials and composites in the practical temperature range from liquid hydrogen to about 3000°F. Consideration is given to fundamental heat transfer processes in characterizing insulation performance in terms of important parameters such as temperature level, gas pressure, and insulation density.

Before considering these characteristics it is helpful to have an idea of how insulation materials are integrated in a structural system. Schematic representations of hot structure and cool or cooled structure systems together with several arrangements of insulative components are shown in Figure 2. Several different approaches for handling the thermal protection problem in the cryogenic to high temperature range are illustrated here. The cool structure system is sized based on insulation requirements for protection of the relatively low temperature primary structure. The hot structure system is sized

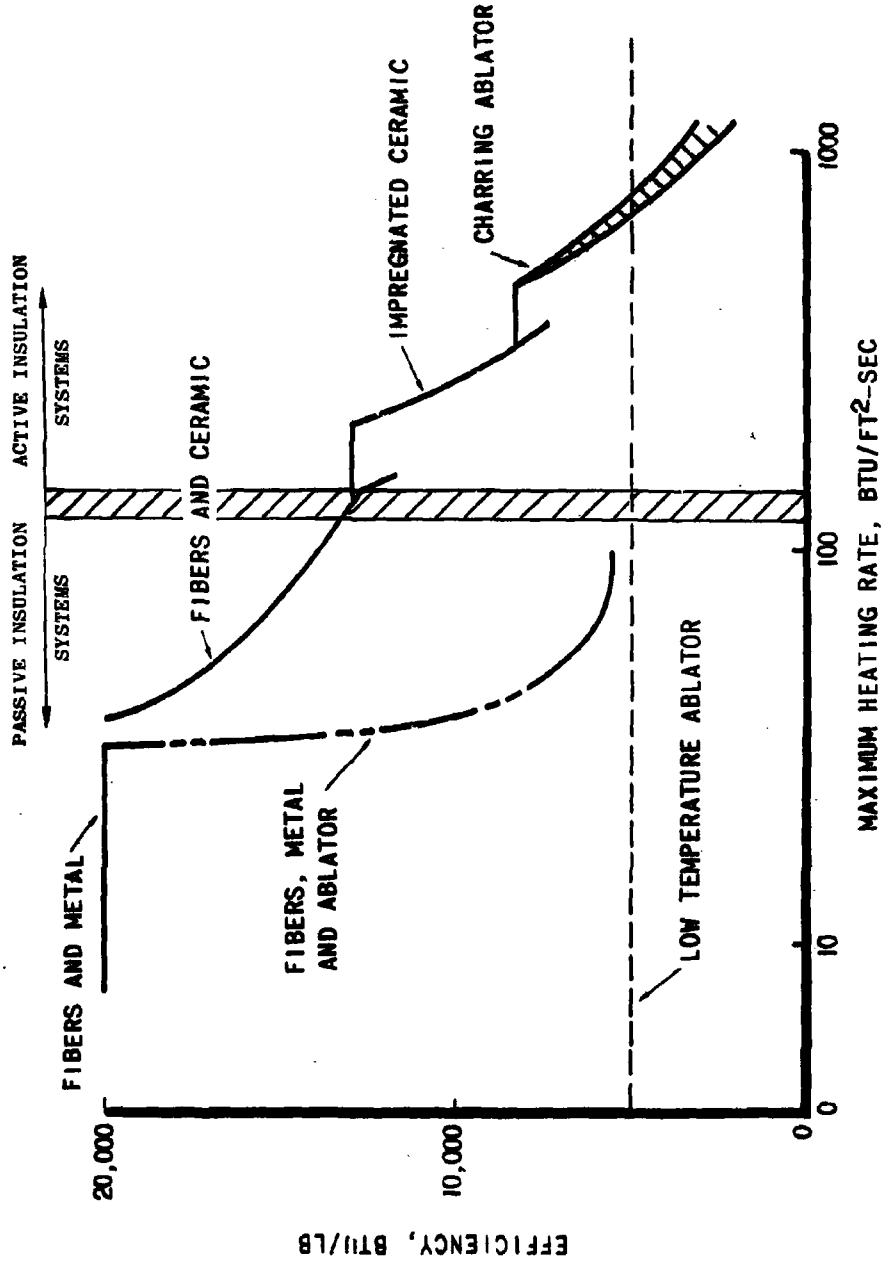

Figure 1. Efficiency of Thermal Protection Systems for an Integrated Heat Load of 50,000 BTU/ft^2

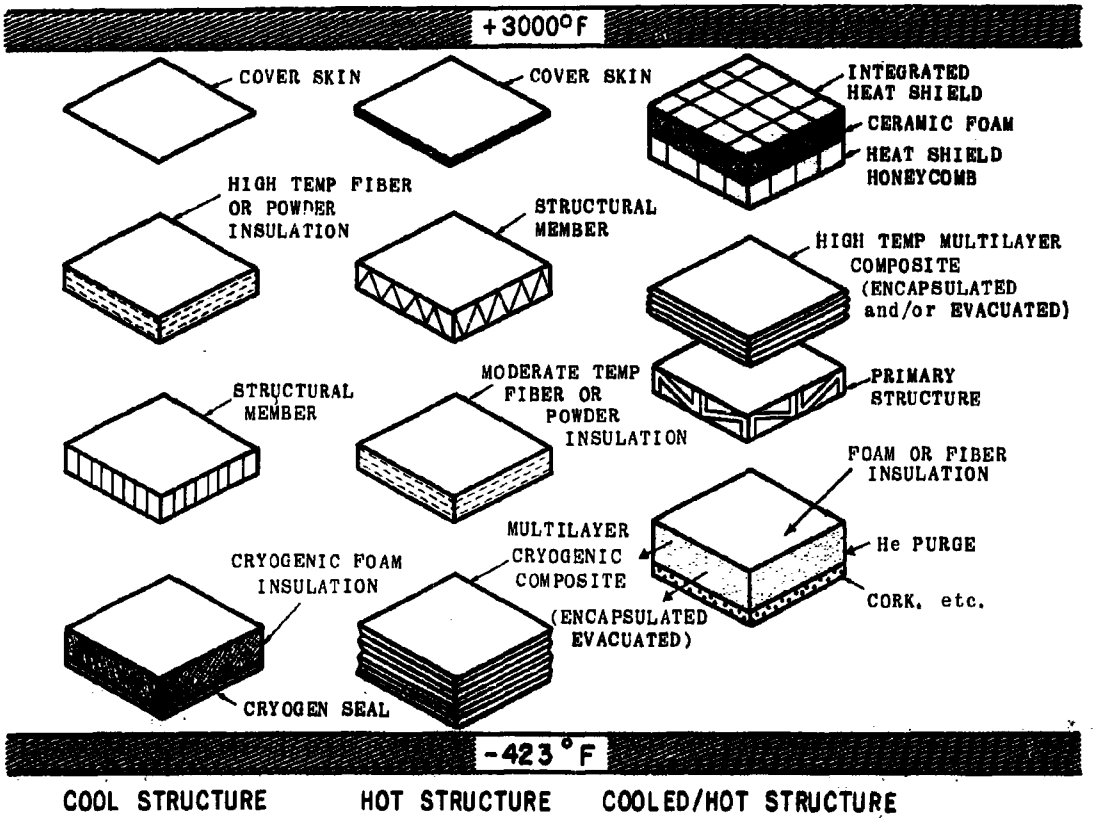

Figure 2. Schematic Representation of Insulation -- Integrated Structures

for protection of fuel and cabin areas, the primary structure being designed to operate at high temperatures. A variation is shown at the right with a high temperature heat shield, with some load-carrying capacity, intermediate insulation, and a relatively low temperature primary structure. The Dyna-Soar system, for instance, incorporates a refractory metal outer skin over fibrous insulation, for protection of a super-alloyed primary structure. Internally, encapsulated and evacuated multilayer insulation is used for cryogenic areas. A somewhat different approach is proposed for systems such as Centaur, where the cryogenic insulation requirements are more critical; organic foams and composites may be considered in these cases.

Many practical problems are encountered in attempting to incorporate various insulation components in an integrated thermal protection system. Heat leaks result when insulation fasteners and mechanical stabilizers are inserted. For liquid hydrogen service, water and air condensation must be eliminated either by evacuation, cryopumping, or helium purge. Another approach as indicated in Figure 2 is to use nonporous insulation (e.g., cork) in the proximity of the hydrogen to raise the effective cold side temperatures above the air condensation point where conventional foam insulations may then be used. In some cases where high temperatures are encountered in the absence of cryogenic cooling (reentry) organic-based insulations cannot be used. In effect, high temperature insulation is added simply to prevent internal temperatures from rising above the decomposition temperature of the organic insulation; system sizing on this basis is, of course, somewhat unrealistic.

Evacuated multilayer insulations, for both cryogenic and high temperature service have very high thermal efficiency because of their radiation attenuation characteristics. In general, these multilayer composites are composed of highly reflective radiation shields (thin gage foil) separated by low conductivity spacer materials such as glass or quartz felt.

However, there are problems associated with their use. Evacuation to relatively high vacuum levels is required for these insulations and thus, encapsulation is necessitated. At high temperatures maintaining a vacuum without active pumping is a difficult task. In some instances lateral thermal conductivity may be up to 10^5 times larger than through conductivity and thus, lateral heat leaks from edge members, structural pinning systems, etc., may become critical. Sensitivity to acoustic vibration, compressive loading, and thermal cycling seem to be prevalent in these higher-efficiency multilayer insulations, and also in powder insulations.

From Figure 2 it is clear that for various passive insulation systems over this temperature range the following physical configurations of materials are encountered: powders, fibers, foams, and multilayer shield composites.

As indicated briefly above, there may be difficult problems encountered when using these materials in practical systems. The purpose of our discussion is to consider these various physical forms of passive insulation, to point out application problems, and to characterize in detail the heat transfer processes occurring. This characterization is in terms of parameters important in weapons system applications such as density, thermal conductivity-temperature level relationships, and effects of interstitial gas pressures. Based on this examination it is possible to understand the underlying problems in developing and perfecting insulation components for the stringent temperature conditions and thus, to have an idea of the direction in which future insulation developments will proceed. Some space will be devoted, also, to an examination of the properties of recently developed insulations.

HEAT TRANSFER PROCESSES

In a discussion of thermal insulation characteristics for flight applications the most important properties are the effective thermal conductivity, expressed throughout this discussion in BTU-in./°F-hr-ft^2 units, and the density in lbs/ft^3 units. The density-thermal conductivity product can be considered as a measure of overall insulation efficiency for a particular material or composite.

In general terms, convection, conduction, and radiation will contribute to overall heat transport and thus to the effective conductance for a particular insulation. The relative contribution of these various modes is extremely important in determining effective conductivity; it is a function of absolute temperature level, insulation geometry, and interstitial gas pressure. It will be assumed here that convective heat transport is negligible. Even at low temperatures where the relative contribution of radiation is small the convective component can be neglected when the interstitial spacing is less than about an eighth of an inch (Ref. 2). For nearly all of the insulations which will be discussed it has been shown experimentally that convective heat transfer can be neglected. The relationship between conduction (solid and gaseous) and radiation can be seen clearly in the following discussion on density effects.

INFLUENCE OF DENSITY

In an examination of conduction and radiation contributions, it is quite apparent that solid conduction will generally increase as the density of the insulation increases while the radiation component will be attenuated as the density increases.

For two semi-infinite parallel planes at steady-state temperatures T_H and T_C, ($T_H > T_C$), Figure 3 (a), the net radiation transfer will of course be

$$(q_o)_{rad} = \epsilon_o \sigma (T_H^4 - T_C^4) \qquad (1)$$

where,

$(q_o)_{rad}$ = steady state radiative heat flux

ϵ_o = emittance of radiating walls (assumed constant)

σ = Stefan-Boltzmann constant

T_H, T_C = hot- and cold-faced temperature, respectively.

Now, if the intervening space is occupied by n parallel radiation shields, Figure 3 (b), it will be desirable to calculate the value of the resultant radiative heat flux $(q_n)_{rad}$ in terms of $(q_o)_{rad}$ for the same overall steady-state temperature difference $(T_H - T_C)$. By writing n radiation heat balances around the n shields for a shield emittance, ϵ_o, the following equations result:

$$(q_n)_{rad} = \epsilon_o \sigma (T_H^4 - T_1^4) = \epsilon_o \sigma (T_1^4 - T_2^4) = \ldots = \epsilon_o \sigma (T_n^4 - T_C^4). \qquad (2)$$

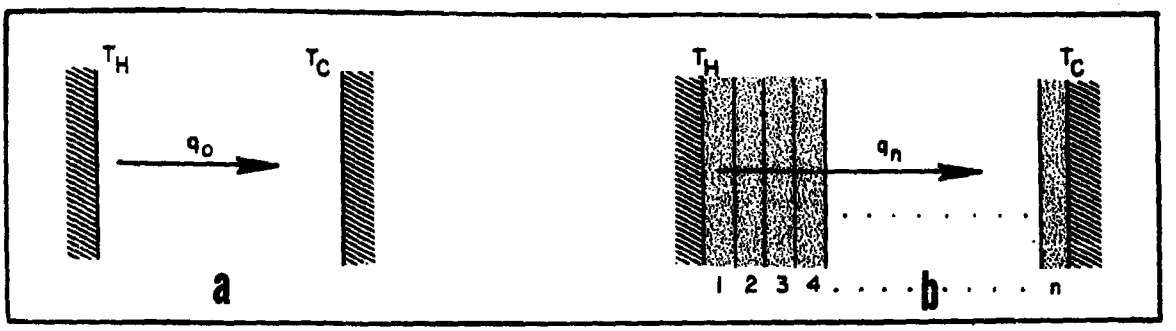

Figure 3. Heat Transfer Between Parallel Planes

If $T_1, T_2, \ldots T_n$ are eliminated from the above equations,

$$(q_n)_{rad} = \frac{\epsilon_o \sigma (T_H^4 - T_o^4)}{(n+1)} = \left(\frac{1}{n+1}\right) q_o \qquad (3)$$

Thus, the overall reduction in steady-state radiation heat transfer is inversely related to the number of shields interposed. The most effective arrangement would, of course, be to suspend the shields in space in a vacuum. In practice, typical multilayer insulations incorporate a low conductivity spacer material such as glass felt or fiber between the shields. With this arrangement the solid conduction contribution is approximately linear in n,

$$q_{cond} \cong C_1 n \qquad (4)$$

where, C_1 is a constant. Equations (3) and (4) are plotted as the dashed-line curves in Figure 4 with the radiation and conduction heat fluxes as a function of the number of shields. Parametric curves in temperature are plotted for $(q_n)_{rad}$. Now if it is assumed, as a first approximation, that the total heat transfer through the insulation is a linear sum of the conduction and radiation contributions (neglecting convection) the overall heat flux q as shown by the family of solid-line curves in Figure 4, exhibits a clear minimum. Note that this minimum occurs at the point where

$$\left|\frac{\partial q_{rad}}{\partial n}\right| = \left|\frac{\partial q_{cond}}{\partial n}\right| \qquad (5)$$

Geometrically, the locus of the minima in the q_T curves in terms of n, the number of shields, is a straight line with slope $2C_1$

$$(q_T)_{min} = 2C_1 n \quad . \qquad (6)$$

As a function of temperature level this minimum total heat flux increases rapidly. The form of this temperature dependence is established as follows:

$$q_T = (q_n)_{rad} + (q)_{cond} = \frac{f(T^4)}{n} + C_1 n \qquad (7)$$

$$\frac{\partial q_T}{\partial n} = C_1 - \frac{f(T^4)}{n^2} \quad . \qquad (8)$$

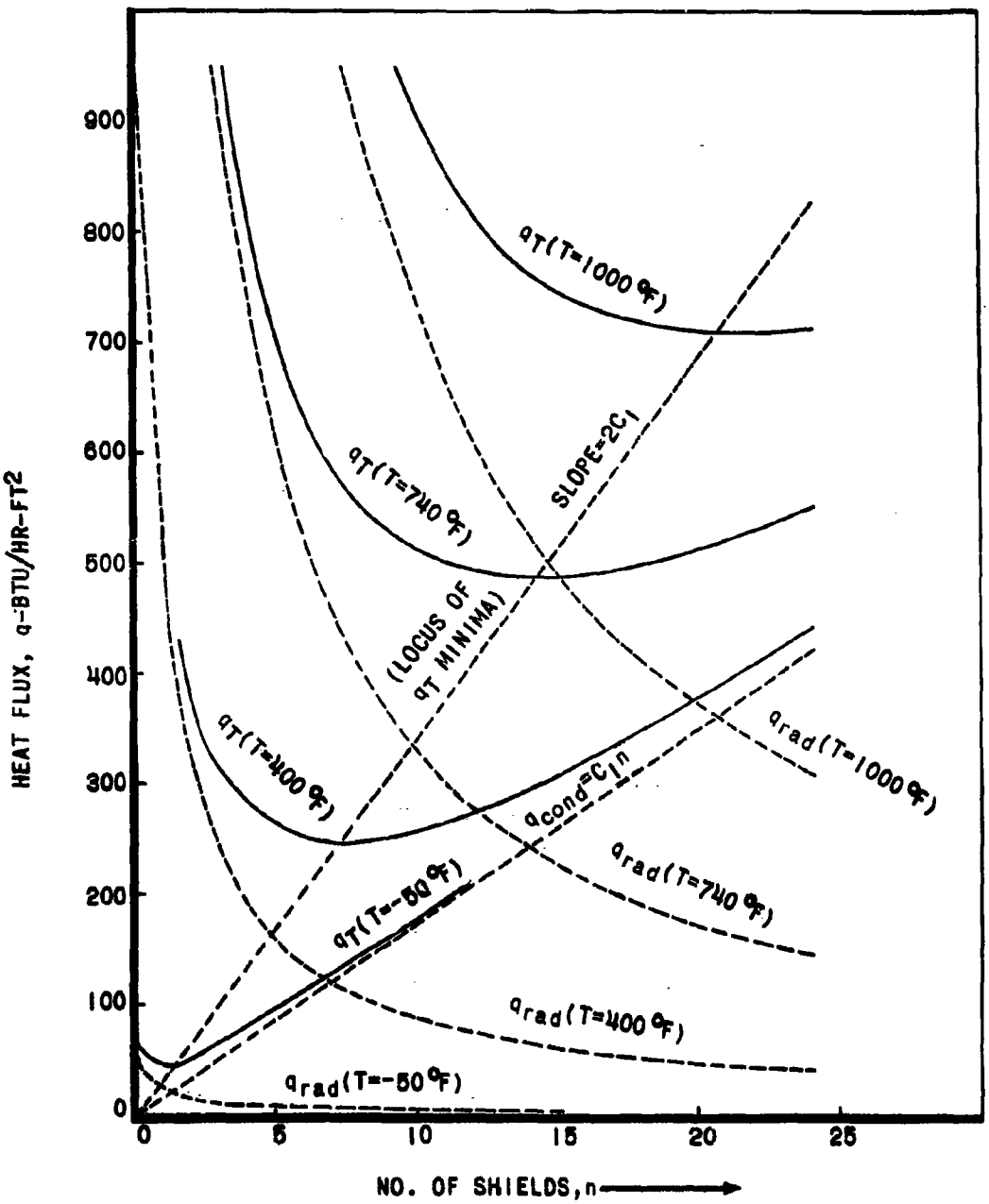

Figure 4. Radiation, Conduction, and Total Heat Flux as a Function of the Number of Shields in a Multilayer Insulation

The value of n when q_T is a minimum, n_{min}, is established from the condition $\partial q_T / \partial n = 0$. Thus,

$$n_{min} = \sqrt{\frac{f(T^4)}{C_1}} \quad . \tag{9}$$

At different temperatures T_1 and T_2

$$\frac{(n_{min})_{T_1}}{(n_{min})_{T_2}} = \frac{\sqrt{f(T_1^4)/C_1}}{\sqrt{f(T_2^4)/C_1}} = \left(\frac{T_1}{T_2}\right)^2 . \tag{10}$$

By combining Equations (6) and (10)

$$\frac{(n_{min})_{T_1}}{(n_{min})_{T_2}} = \frac{(q_{T_{min}})_{T_1}}{(q_{T_{min}})_{T_2}} = \left(\frac{T_1}{T_2}\right)^2 . \tag{11}$$

The significance of this is:

1. The total heat flux exhibits a minimum as a function of the number of shields.

2. As the overall temperature level rises the minimum heat flux obtainable also rises and shifts toward higher n values.

The same type of functional relationship between q_{rad}, q_{cond} and q_T is also exhibited by foams, fibers, and powders where the independent variable is the insulation density (in a multilayer insulation the number of shields, n, per unit thickness is, of course, proportional to the density). This characteristic is expected since radiation attenuation is achieved at the expense of increased solid conduction and increased weight. Observe that since the minimum conductivity and corresponding density both increase with temperature, the thermal efficiency parameter ($k \times \rho$) will increase even more rapidly with temperature.

Experimentally observed variations in effective thermal conductivity with density (and number of shields for a multilayer insulation) are shown in Figure 5 for typical foam, fibers, powders and a common "super insulation," aluminized and crinkled polyester film. Note that the thermal conductivity ordinate for the aluminized film is logarithmic and that the curve rises rapidly after the n_{min} is reached. This indicates one of the important practical limitations of multilayer composites, that insulation performance is quite sensitive to compressive loading and degrades rapidly under moderate compression.

INFLUENCE OF INTERSTITIAL GAS PRESSURE -- GAS CONDUCTIVITY

Because of gaseous conduction the interstitial gas pressure has an important influence on the effective thermal conductivity of the basically porous insulations being considered here. Kinetically, the laminar gas transport parameters for momentum and thermal energy, viscosity and thermal conductivity, respectively, can be considered as equivalent.

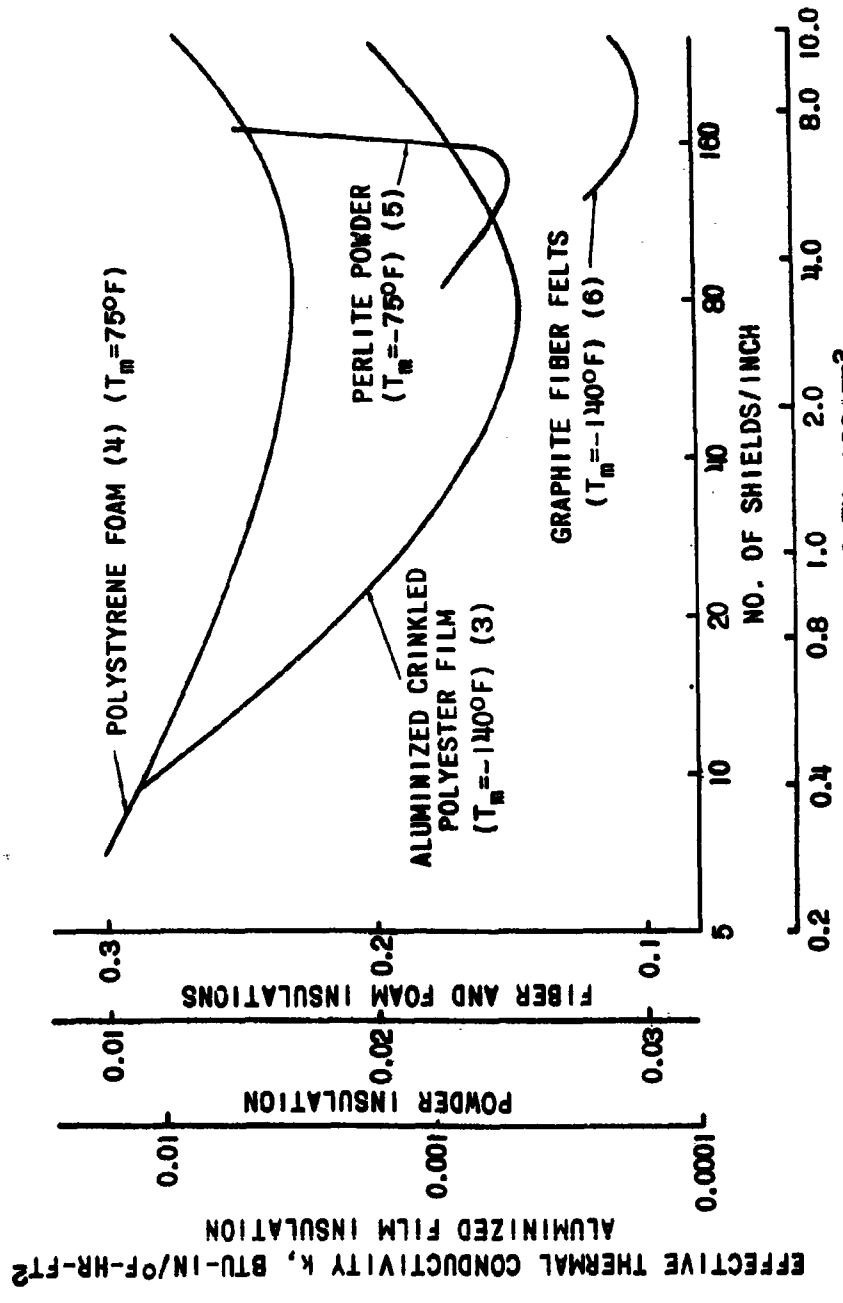

Figure 5. Effective Thermal Conductivity as a Function of Insulation Density (NOTE: Numbers in parentheses pertain to numbered references.)

That is, the same basic molecular movement is responsible for both shear stress development (viscosity effects) and net heat transport. It is an important and a well-known result of kinetic theory that at moderate pressures gas viscosity is independent of pressure but increases rapidly with increase in temperature. Because of the similar transport processes involved the same holds true for gaseous thermal conductivity.

The following results can be written from kinetic theory relating thermal conductivity, viscosity, temperature, and molecular weight of the gaseous species (Ref. 7).

$$k_g = \frac{1}{3} V \lambda C_v = C_1 \lambda \tag{12}$$

$$V = C_2 \sqrt{\frac{T}{M}} \tag{13}$$

$$\eta = \frac{C_3 T^{3/2}}{C_4 + T} \tag{14}$$

where,

k_g = gaseous thermal conductivity

V = mean particle speed

η = viscosity

C_v = specific heat

λ = mean free path

C_1, C_2, C_3, C_4 = constants.

Thus, gaseous thermal conductivity increases with temperature and is inversely related to the molecular weight of the gas. Typical curves illustrating these relationships for helium, air and CO_2 are shown in Figure 6.

The gaseous thermal conductivity is independent of pressure at moderate pressure levels because the molecular mean free path is inversely proportional to pressure while the density is directly proportional to pressure, thus cancelling the pressure effects. As far as energy transport is concerned, when the mean free path λ becomes comparable to the interstitial spacing with the insulation, d, as a result of pressure reduction, the insulation in effect imposes a constant mean free path on the molecules, $\lambda = d$. Thus, for $\lambda \geq d$ the gaseous conductivity becomes pressure dependent, decreasing as the pressure is reduced.

These pressure effects on insulation conductivity for various foams, fibers, powders, and multilayer insulations are shown in Figure 7. The curves exhibit the behavior expected in insulations where the gas phase is continuous. Further, note that the thermal conductivity ordinate is logarithmic and thus the effect is quite pronounced particularly in the case of the more efficient multilayer and powder insulations. The curves flatten at low pressure where the solid conduction contribution is constant and the gaseous conduction contribution is negligible. In these curves air was the interstitial gas; if helium were employed the pressure independent regions would, of course, be shifted upward by a large amount.

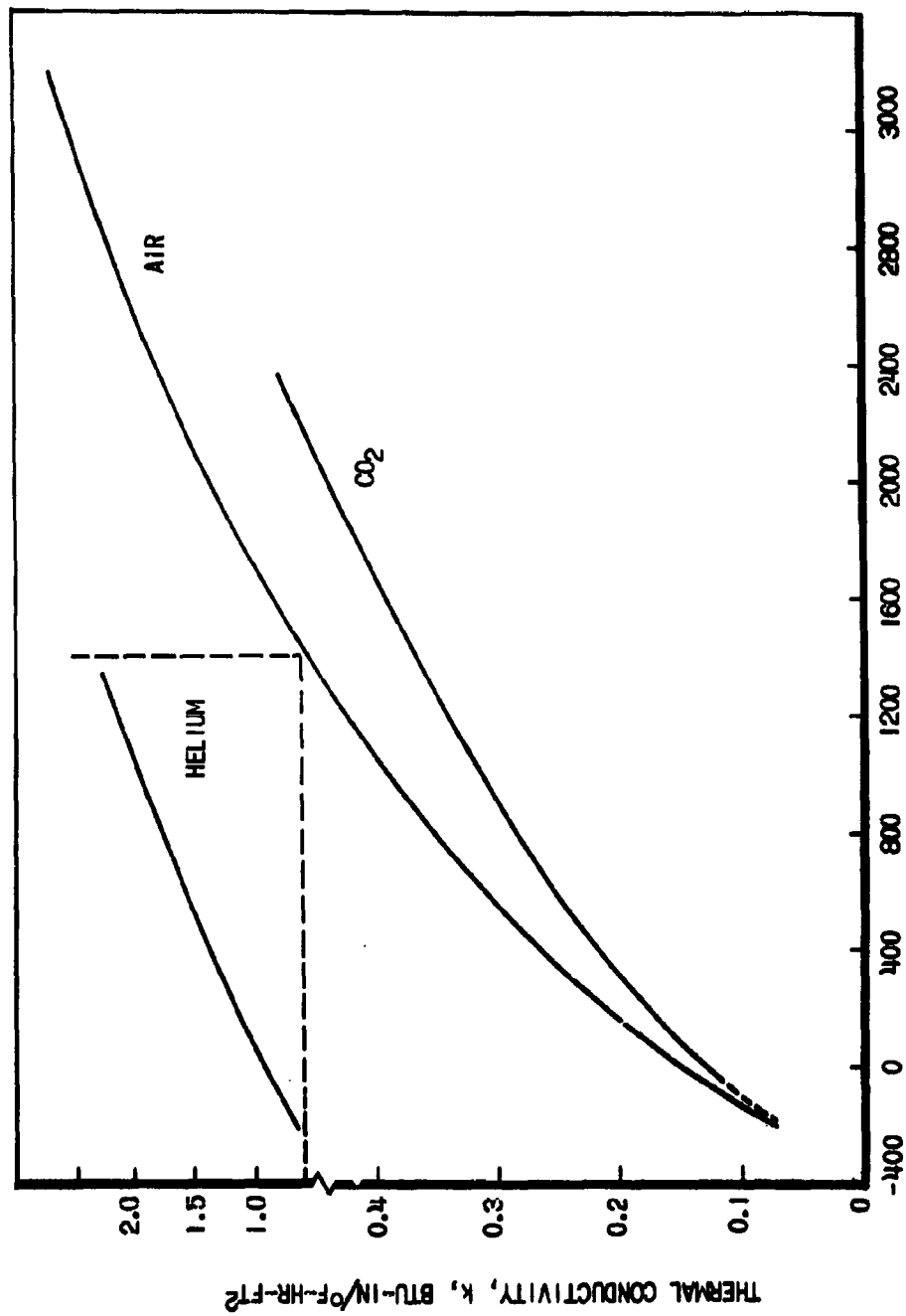

Figure 6. Thermal Conductivity of Various Gases (Ref. 8)

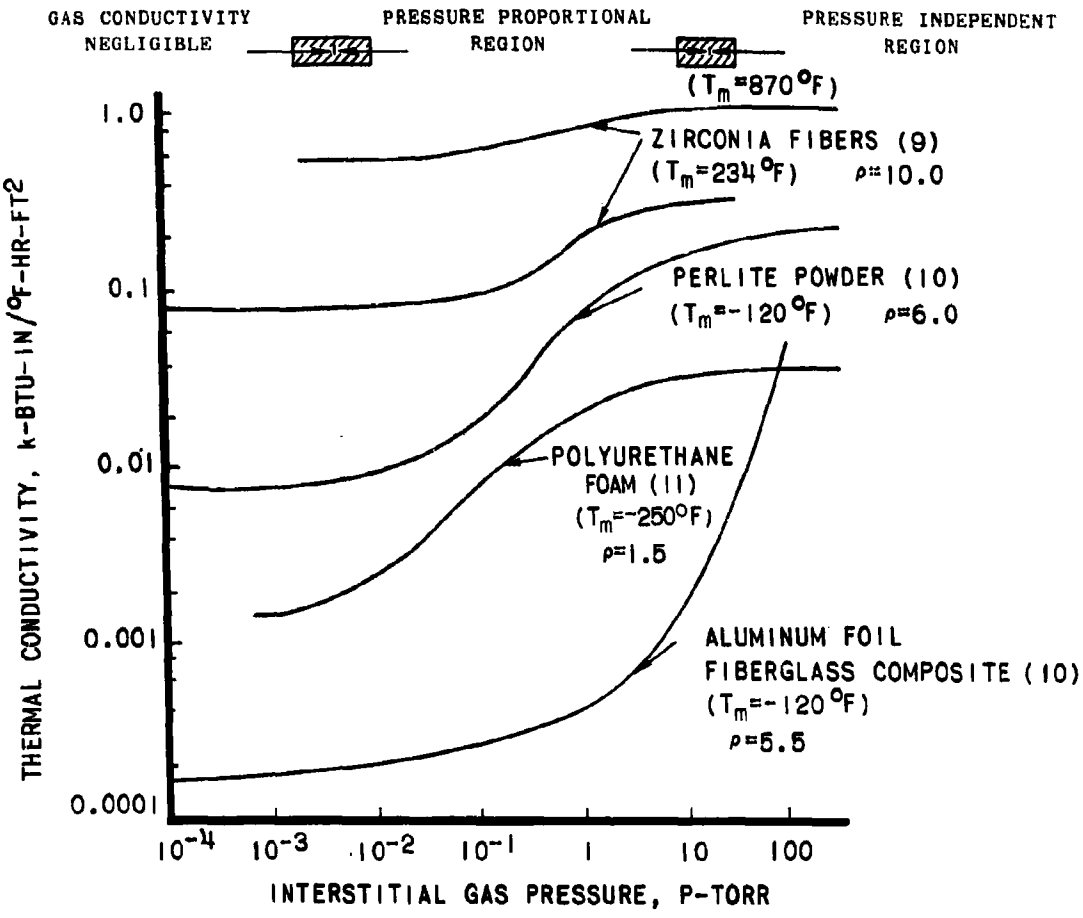

Figure 7. Effect of Interstitial Gas Pressure on Effective Thermal Conductivity of Various Insulations
(NOTE: Numbers in parentheses pertain to numbered references.)

With the use of CO_2 this region would be depressed. Hence, variation of the gaseous species can be used to control effective conductivity to some extent.

As shown above, a significant reduction in gas conductivity can be obtained by increasing λ to the order of the interstitial spacing, d. This is most readily accomplished by pressure reduction. Another method for accomplishing the same result is to work at atmospheric pressure and reduce the interstitial spacing such that $d = \lambda_{ap}$, where ap is atmospheric pressure. Very small spacing is required since at one atmosphere $\lambda \cong 0.1\mu$. This principle has been successfully employed without deleterious density increases in commercial "Min-K" insulations developed by Johns-Manville. Observed thermal conductivity values are approximately 40 percent that of still air (Ref. 12).

If gas conductivity contributions are considered as a function of temperature level, it is clear from Figure 6 that there is a general increase which is approximately linear.

Now, for a given overall temperature difference the radiation contribution is approximately cubic in temperature and thus, as the absolute temperature level increases, the relative contribution of gas conductivity decreases. It is important to note that near room temperature the gas conduction component is the major contribution to the overall heat transfer. This is true also at cryogenic temperatures to the condensation temperature of the gas. For typical nonevacuated cryogenic insulations (e.g., organic foams) the natural lower limit for the effective conductivity is that of the interstitial gas. As shown above, this gas conductivity contribution can be decreased to some extent by using high molecular weight gases in closed foams. Thus, as expected, a typical freon-blown polyurethane foam exhibits good insulating characteristics. If the gas contributions are eliminated through evacuation, radiation transfer will predominate and will require a multilayer shield composite for effective radiation attenuation. This approach is generally used in all cryogenic super insulations.

SOLID CONDUCTION AND RADIATION HEAT TRANSFER -- INFLUENCE OF TEMPERATURE

With the conclusion of the discussion on effects of gaseous conductivity, one major factor remains to be considered -- the influence of solid conduction and radiation on the net heat transport in the insulation.

Solid Conduction

There are basically two physical configurations to consider in examining the effects of solid conduction. The first is the case where the solid phase is continuous, as in typical foams; the second is where the solid phase is discontinuous, as in powders and fibers. As pointed out by Klein (Ref. 13) there is a profound effect on overall thermal conductance on shifting from a system where the solid phase is continuous to one where the solid phase is discontinuous but the gas phase is continuous. If the solid phase is continuous, the overall thermal conductivity is characteristic of the solid. The effect of the relatively high resistance void volume is only a decrease in the effective conductivity in proportion to the void fraction, as shown in Equations (15), (16), and (17). When the solid phase is discontinuous a high thermal contact resistance is interposed in series and thus the effects of the high resistance voids may predominate.

These characteristics lead to fundamentally different forms for the equations for solid conduction in foams as compared with the equations for fibers or powders. In continuous solid phase materials, such as foams, the thermal resistances are essentially in parallel and the conduction equation (Ref. 4) becomes:

$$k_{cond} = V_{solid}\, k_{solid} + V_{gas}\, k_{gas} \tag{15}$$

or,

$$k_{cond} = k_{gas} + \frac{\rho_{insulation} - \rho_{gas}}{\rho_{solid} - \rho_{gas}} \left(k_{solid} - k_{gas}\right) \tag{16}$$

where,

k = thermal conductivity

V = volume fraction

ρ = density.

When $k_{solid} >> k_{gas}$

$$k_{cond} = \nu k_{solid} \tag{17}$$

where,

$$\nu = 1 - (\text{void fraction}).$$

Thermal conductivity values for various foams covering the -400° to +3000°F temperature range are shown in Figure 8. The thermal conductivities of the various bulk solids are also presented, from which we can see that the thermal characteristics of the continuous solid phase do establish the level of foam conductivity. The SiO_2 curve increases rapidly with temperature as a result of the diathermanous behavior (radiation transparency) of the silica at higher temperatures.

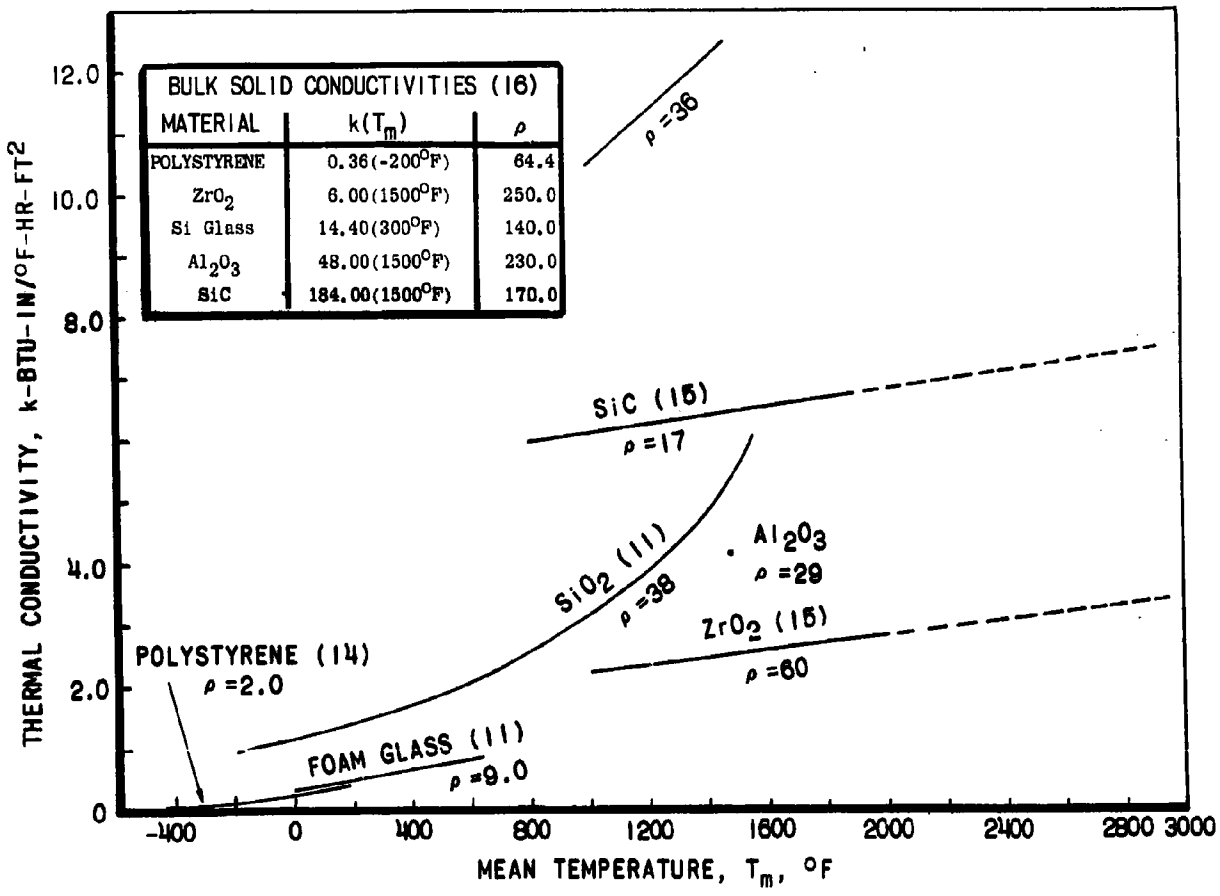

Figure 8. Thermal Conductivity of Foams
(NOTE: Numbers in parentheses pertain to numbered references.)

For the solid conduction contribution in materials with a discontinuous solid phase, the inter-particle or inter-fiber contact area and associated contact resistance tends to be the controlling factor. Generally, the equations developed are based on contact areas which are assumed to be formed through elastic deformation. For equi-diameter spheres (powders) or mutually perpendicular cylinders (fibers) deforming elastically the area of contact is given (Ref. 17) as,

$$A_{concact} = \pi \left[\sqrt[3]{\frac{3}{4} \frac{P(1-\mu)^2 R}{E}} \right]^2 \tag{18}$$

where,

μ = Poisson's ratio

E = modulus of elasticity

R = particle radius

P = load, lbs = $F/n^2 = 4R^2$

F = load/unit area

n = number of spheres/unit volume .

By using the above expression the effective solid conductivity for open-packed powders as determined by Glaser, et al. (Ref. 18) becomes:

$$(k_{cond})_{powder} = \frac{3}{8} \pi k_{solid} \left[\frac{3}{E} (1-\mu^2) F \right]^{4/3}. \tag{19}$$

For fibers (Ref. 19), the equation is

$$(k_{cond})_{fibers} = \frac{(k_{solid})(4\pi R^2 n)}{R_f + \ell n \left[\frac{A_{fiber}}{A_{contact}}\right] + 1} \tag{20}$$

where,

l = distance between fiber junctions.

Thus, for powders, the solid conduction contribution is proportional to k_{solid} and increases with the applied load but is independent of the size of the spheres for this simple case. For fibers, the solid conduction contribution is again proportional to k_{solid} but is inversely related to the fiber radius and the number of inter-fiber contacts. As expected, insulations of small-diameter fibers of low density exhibit the lowest solid conduction. Fibers appear to be less sensitive to compressive loading than are the powders; also, the larger number of contacts/unit volume present in a powder insulation makes them more sensitive to sintering, which may become severe at high temperatures.

Radiation Transport

The process of radiant heat transfer in insulating materials is extremely complex. Closed-form evaluation of geometric radiation interchange factors is, of course, impossible. The somewhat empirical approach of writing the overall radiant heat transport

equation in terms of absorption, reradiation, and scattering coefficients has proved successful and to some extent reflects the actual physical radiation attenuation processes occurring in the material. It is assumed, first, that the net one-dimensional heat flux can be resolved into two components, one component traveling in the direction of the temperature gradient, the second in the opposite direction (Ref. 20). An overall heat balance for these two radiation components is then written in terms of absorption and scattering coefficients (Ref. 18). The final equations can be written:

$$\frac{dI_2}{dX} = -(N+P)I_2 + NI_2 + PJ^2\sigma T^4 \tag{21}$$

$$\frac{dI_1}{dX} = -(N+P)I_1 + NI_1 + PJ^2\sigma T^4 \tag{22}$$

$$q_{rad} = I_2 - I_1 \tag{23}$$

where

I_1, I_2 = integrated radiation heat flux in the positive and negative directions, respectively

q_{rad} = net radiation heat flux

N = scattering cross section

P = absorption cross section

J = index of refraction.

If boundary conditions with the insulation contained between two parallel surfaces with emittance E_o at X = O and X = L are applied, the overall radiant flux as derived by Glaser (Ref. 18) becomes

$$q_{rad} = \frac{J^2\left(T_o^4 - T_L^4\right)}{(P+2N)\frac{L}{2} + \frac{2}{\epsilon_o} - 1} . \tag{24}$$

Incorporation of radiation attenuation and scattering media (increasing P and/or N) can be effective in reducing net heat transfer by radiation. This is particularly true at high temperatures where q_{rad} is relatively large. Note, however, that the fourth power relationship in temperature still exists as in the case when radiation shields are incorporated. See Equation (3).

Thermal conductivity curves as a function of temperature for several recently developed fibrous and powder insulations are presented in Figure 9. All curves are for the insulations in a vacuum environment. In general, the powders exhibit conductivities of a lower level than the fibrous insulations. In a transverse path through the insulation in the direction of the temperature gradient the powders and fibers present the same basic heat flow resistance-point contact of highly curved surfaces. Laterally, the powders present this same high resistance geometry, but the fibrous insulations present a relatively low resistance solid conduction path axially along each fiber. Because heat transfer in both of these directions is required for a net flux, with respect to the temperature gradient, the lower effective conductivities for the powders is expected.

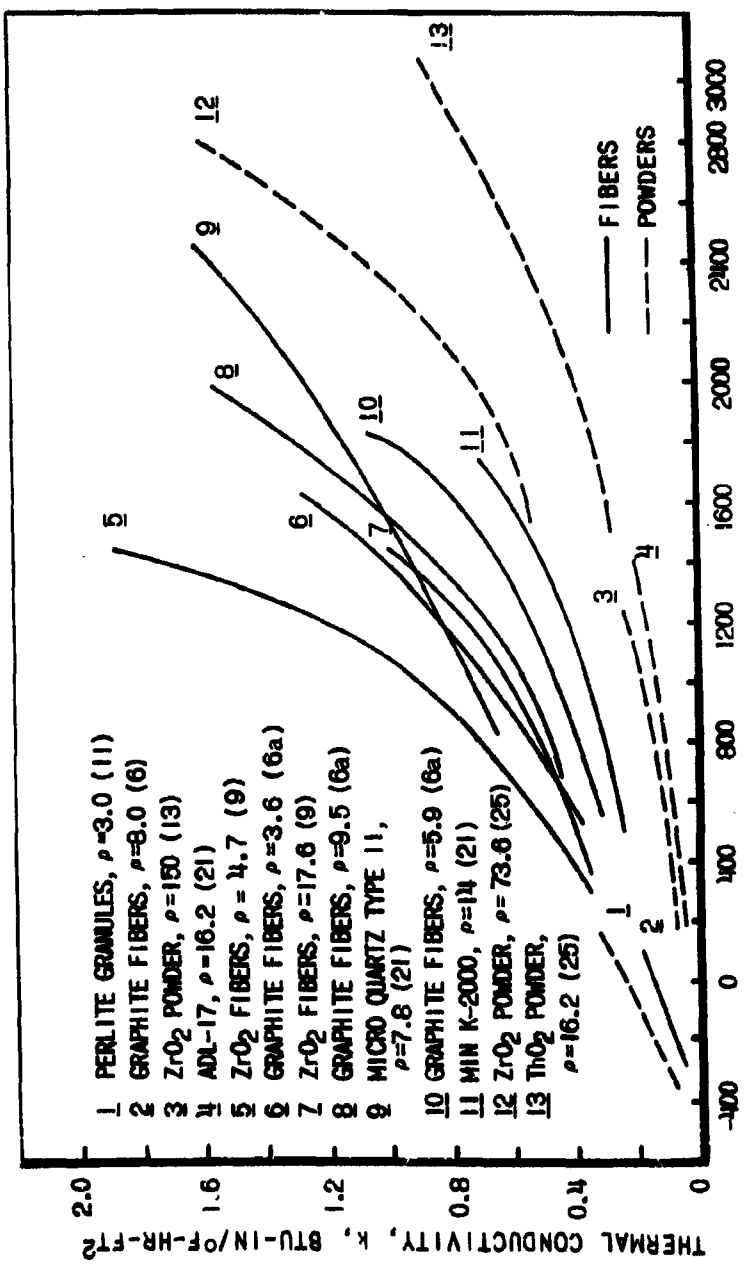

Figure 8. Thermal Conductivity of Fibers and Powder
(NOTE: Numbers in parentheses pertain to numbered references.)

Applications of the principles discussed above in improvement of insulation efficiency are found in such insulations as ADL-17 where opacifiers and thermal resistance components are incorporated to reduce the effective conductivity. This particular insulation is composed of Al_2O_3, fibrous asbestos, silicon nitride, carbon powder and aluminum flakes. Density effects are clearly seen in the graphite fiber curves of Figure 9. Densities near 6.0 lbs/ft^3 appear to be optimum with both the high density (ρ = 9.5) and the low density (ρ = 3.6) fibers exhibiting higher conductivity than the 5.9 density fibers. The important influences of radiation relative to solid conduction is noticeable in the ZrO_2 fiber curves where large increases in density (from 4.7 to 17.6) still produce large decreases in conductivity. The efficiency of the Min-K insulation through void dimension reduction is also apparent. A curve for Microquartz, Type II, one of the more promising high temperature, oxidizing environment insulations is also shown. In the high temperature region this insulation appears to be among the best of the fibrous-based materials.

CONCLUDING REMARKS

After the above discussion of the important physical processes influencing the various heat transport modes in the several classes of insulations, it now remains to compare their relative performance in terms of the overall efficiency criteria: conductivity, k, density, ρ, and the product (ρ x k). From a practical viewpoint some indication has already been given of the considerations involved in insulation applications for high performance vehicles. In the comparisons that follow the more critical application problems will be touched upon again.

The comparison between typical foams, fibers, powders, and some of the more promising evacuated multilayer shield composites is given in Figure 10 and Table 1; note that the conductivity ordinate is logarithmic. The air conductivity curve is shown also for reference. Clearly, now that the thermal conductivity curves for the multilayer shield composites in Figure 10 are in vacuum environment, the extremely high thermal efficiency would be completely lost if gaseous conduction were present. This characteristic is, of course, more pronounced at the lower temperature levels where radiation attenuation is highly effective. From Equations (3) and (24), even with the incorporation of absorption, scattering media, and radiation shields for a given overall temperature difference, the radiation transport is still cubic in temperature. Thus, in no case is it possible to effect a reversal of the trend of increasing effective insulation conductivity with increasing temperatures. This generalized trend toward radiation predominance, irrespective of physical geometry, can be used to explain the fact that, at high temperatures, insulation conductivities range over slightly more than an order of magnitude while at cryogenic temperatures the variation may be over several orders of magnitude as shown in Table 1.

An additional factor of fundamental importance must be considered, particularly in the use of insulations for high temperature service. This is the question of inter-material compatibility, insulation stability, and, in turn, the attendant problem of thermal protection system reliability. The highly efficient Linde super insulation shown in Figure 10 with nickel foil shields is obviously temperature limited. Similarly, in the case of the A.D. Little multilayer insulation, consideration must be given not only to compatibility between the tantalum, graphite, and the ADL-17, but also to the fact that the refractory metal and the graphite are highly susceptible to oxidation. Encapsulation and evacuation could be used to prevent oxidation and at the same time eliminate gas conduction. With both powders

and multilayer insulations significant heat leaks and weight penalties may be involved. And then, of course, there is the question of finding a suitable material for the encapsulation system itself. It should be clear that the vacuum required with powder insulations is less extreme than with multilayer insulations (Ref. 27). This is due to the fact that the interstitial spacings in powdered materials are generally smaller and a lesser vacuum is required to produce a molecular mean free path comparable to the size of the interstitial spacings. Although the density values of multilayer composites are favorable, the weight penalty of the encapsulation and evacuation components are not included here. If typical high efficiency foam insulations were considered as shown in Figure 10, relatively high conductivity values would be exhibited at all temperature levels. Because of the practical limitations encountered in the use of evacuated multilayer and powder insulations and the high conductivity levels of foam materials, fibrous insulations are presently in widest use.

Although easier to use, the fibrous insulations are definitely of lower thermal efficiency. In some current applications thermal protection with fibrous insulations has not been perfected. This is due in part to the fact that, from an overall system performance viewpoint, thermal protection has not been a critical factor in these vehicles. In many of the systems envisioned for the future, thermal protection will become a much more critical factor, and furthermore, multimission reliability will be demanded of components used for that purpose. The present state-of-the-art does not satisfy many of these requirements. Further developments and improvements in thermal efficiency and overall reliability of nonevacuated composites, particularly systems incorporating radiation shield networks are certainly warranted. Advancement is most likely to appear first in encapsulation and evacuation of high temperature insulation because of their high efficiency.

The problem at cryogenic temperatures is somewhat reduced in the case of evacuated systems since outgassing stability problems do not arise. Further, effective use of cryopumping can be made. Relatively speaking, evacuation is much more essential for effective cryogenic insulation performance than for effective insulation at high temperatures. Because of the less severe practical problems, the cryogenic super insulations find wider application. Considerable improvements must be made, however, in heat leak reduction, particularly when large surface areas are encountered as in cryogenic tankage.

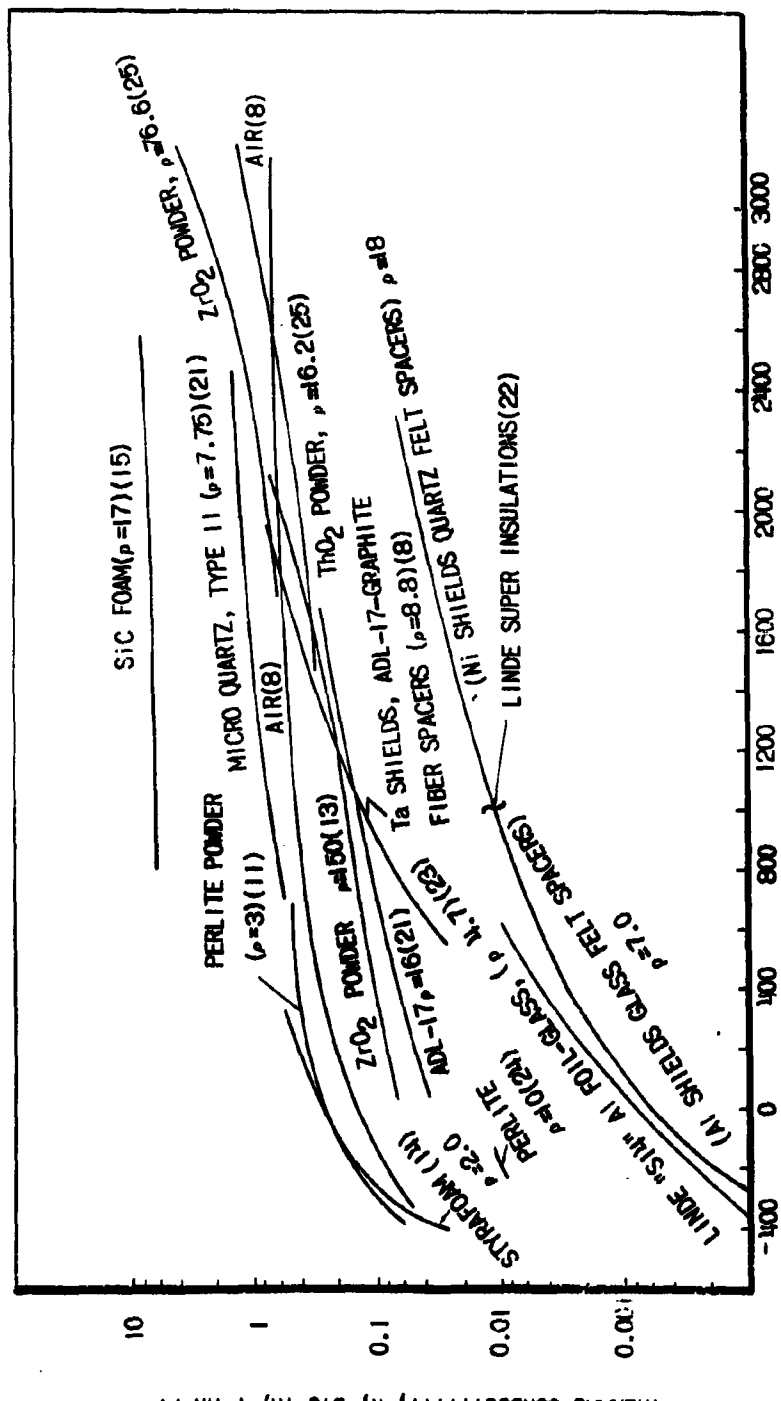

Figure 10. Comparison of Foam, Fiber, Powder and Multilayer Insulations: -400° to +3000°F
(NOTE: Numbers in parentheses pertain to numbered references.)

TABLE 1. TYPICAL PROPERTIES OF VARIOUS THERMAL INSULATIONS

CRYOGENIC - T_m = -250°F				HIGH TEMPERATURE T_m = 2000°F			
Insulation	Thermal Conductivity $\left(\frac{\text{BTU-in.}}{°\text{F-hr-ft}^2}\right)$	Density (lbs/ft^3)	Conductivity Density Product	Insulation	Thermal Conductivity $\left(\frac{\text{BTU-in.}}{°\text{F-hr-ft}^2}\right)$	Density (lbs/ft^3)	Conductivity Density Product
Organic Foam	1×10^{-1}	2.0	2.0×10^{-1}	Foam (SiC)	7.0	17	119
Fibrous Insulation (Evacuated)	0.10	7.0	7×10^{-1}	Quartz Fibers (Evacuated)	1.5	3.5	5.3
Air	7×10^{-2}	0.2	1.4×10^{-2}	Air	0.6	0.017	1.02×10^{-2}
Evacuated Powder	8×10^{-3}	6.0	4.8×10^{-2}	Evacuated Powder (Al_2O_3)	2.6	100	260
Multilayer Composite (Evacuated)	3×10^{-4}	4.7	1.4×10^{-3}	Multilayer Composite (Evacuated)	0.24	9.5	2.38

REFERENCES

1. Heldenfels, R. R., "Structures for Manned Entry Vehicles," Conf. on Aerodynamically Heated Structures, Prentice Hall, Inc., Englewood Cliffs, N. J. (1962).

2. King, W. J., Mech Engr, 54, 347-353 (May 1932).

3. Black, I. A., et al., Liquid Propellant Losses During Space Flight, 6th and 7th Quarterly Progress Reports, Contract NAS5-664 (September 1962).

4. Guenther, F. O., S P E Trans, 243-249 (July 1962).

5. Everest, A., Glaser, P. E., and Wechsler, A. E., Thermal Conductivity of Non-Metallic Materials, Summary Report, Contract NAS8-1567 (April 1962).

6. Wechsler, A. E., Thermal Properties of High Temperature Insulation Materials, Third Quarterly Progress Report, Contract AF 33(657)-9172, WPAFB, Ohio (February 1963).

6a. Ibid., Monthly Report No. 11 (April 1963).

7. Dushman, S., Scientific Foundations of Vacuum Technology, John Wiley and Sons, Inc., New York (1949).

8. Hilsenrath, J., et al., Tables of Thermal Properties of Gases, NBS Circular 564 (Nov 1955).

9. Adams, J. J. and Sterry, J. P., Synthesis of Light Weight Insulation, Second Quarterly Progress Report, Contract AF 33(657)-8902, WPAFB, Ohio (January 1963).

10. Glaser, P. E., Thermal Protection Systems for Liquid Hydrogen Tanks, Contract NAS5-664 (November 1962).

11. Moeller, C. E., Loser, J. B., Synder, W. E., and Hopkins, V., Thermophysical Properties of Thermal Insulating Materials, ASD-TDR-62-215, WPAFB, Ohio (July 1962).

12. Johns-Manville Company, Bulletin No. IN-254A (1959).

13. Klein, J. D., Heat Transfer by Radiation in Powders, Ph.D. Thesis, M.I.T. (June 1960).

14. Haskins, J. F. and Hertz, J., "Thermal Conductivity of Plastic Foams from -423°F to 75°F," Adv Cryo Eng, 7, 353-359 (1962).

15. Carborundum Co., Adv Materials Tech, 3, No. 2 (June 1960).

16. Goldsmith, A., Waterman, T.E., and Hirschhern, H. J., Thermophysical Properties of Solid Materials, WADC-TR-58-476, WPAFB, Ohio (August 1960).

17. Timoshenko, S. and Goodier, J. N., Theory of Elasticity, McGraw-Hill Book Co., Inc., New York (1951).

REFERENCES (CONT'D)

18. Glaser, P. E., et al., Investigation of Materials for Vacuum Insulation up to 4000°F, ASD-TDR-62-88, WPAFB, Ohio (January 1962).

19. Strong, H. M., Bundy, F. P., and Borenkerk, H. P., J. Appl Phys, 31, 39 (1960).

20. Hamaker, H. C., Philip Res Report, 2, 55, 103 (1947).

21. Lange, R. A., Light Weight Thermal Protection System Development, Quarterly Progress Report No. 2, Vol I., Contract AF 33(657)-9444, WPAFB, Ohio (January 1963).

22. Lindquist, C. R., Linde Company Super Insulation Applied to Space Vehicles (December 1962).

23. Riede, P. M., Wang, D. I-J., "Characteristics and Applications of Some Super Insulations," Adv Cryo Engr, 5, D-4, 209-215 (1960).

24. Black, I. A., Fowle, A. A., and Glaser, P. E., "Development of High-Efficiency Insulation," Adv Cryo Engr, 5, 181-188 (1960).

25. Wechsler, A. E., and Glaser, P. E., Investigation of Thermal Properties of High Temperature Insulation Materials, ASD-TDR-63-574, WPAFB, Ohio (July 1963).

26. Anderson, R. A., and Swann, R. T., Structures for Re-entry Heating, NASATMX-313 (September 1960).

27. Kropschot, R. H., Applied Cryogenic Engineering, 152-69, John Wiley & Sons, Inc., New York (1962).